

Renormalization flow towards gravitational catalysis in the $3d$ Gross-Neveu model

Holger Gies and Stefan Lippoldt

Theoretisch-Physikalisches Institut, Friedrich-Schiller-Universität Jena, Max-Wien-Platz 1, D-07743 Jena, Germany

Catalyzed symmetry breaking arises from a parametric enhancement of critical fluctuations independently of the coupling strength. Symmetry-breaking fermionic long-range fluctuations exhibit such an enhancement on negatively curved spaces, as is known from mean-field studies. We study gravitational catalysis from the viewpoint of the functional renormalization group using the $3d$ Gross-Neveu model as a specific example. We observe gravitational catalysis towards a phase of broken discrete chiral symmetry both on a maximally symmetric (AdS) and on a purely spatially curved manifold for constant negative curvature (Lobachevsky plane). The resulting picture for gravitational catalysis obtained from the renormalization flow is closely related to that of magnetic catalysis. As an application, we estimate the curvature required for subcritical systems of finite length to acquire a gravitationally catalyzed gap.

I. INTRODUCTION

Mass gap generation and (chiral) symmetry breaking in relativistic fermionic systems can arise from a variety of mechanisms which are often related to certain couplings or interaction channels becoming dominant. An apparent counter-example is catalyzed symmetry breaking, first studied in the context of magnetic catalysis [1–3], where mass gap generation is triggered by the presence of a magnetic field even for arbitrarily small values of the interaction strength. This phenomenon can be understood in various ways, the essence being that the long-range fluctuations driving the symmetry-breaking transitions are parametrically enhanced, see [4] for a recent review. More concretely, a magnetic field induces a fermionic fluctuation spectrum with Landau-levels containing a zero mode that leads to an enhancement of the density of states in the IR and to an effective dimensional reduction favoring symmetry breaking. Magnetic catalysis has found a rich variety of applications both in particle physics (chiral phases of QCD) [5–11] and condensed matter physics [12–18].

Another simple picture for magnetic catalysis has recently been developed within the framework of the functional renormalization group in the context of the $3d$ Gross-Neveu model [19]. In line with the fact that symmetry-breaking phase transitions are often related to fixed points of renormalization group transformations, also magnetic catalysis can be related to the behavior of RG fixed points as a function of the magnetic field. This RG picture has already successfully been applied in the context of QCD [20].

In the present work, we verify the underlying RG picture of catalyzed symmetry breaking in the context of curved spacetimes. The fact that symmetry breaking and mass generation in fermionic systems can be influenced by negative curvature of the spacetime has been realized early [21], and is meanwhile reviewed in textbooks [22]. The phenomenon is typically studied at mean-field level and occurs in many different fermionic models [23–35]. In [36], the similarity to magnetic catalysis was realized in terms of an effective dimensional reduction mechanism

of the spectral properties of the Dirac operator. This justifies the use of the terminology “gravitational catalysis” [37].

In fact, we find in the present work that the effective dimensional reduction and the corresponding enhancement of the density of states in the IR is directly related to the fixed point structure as identified below. From this RG viewpoint, symmetry breaking arises as a consequence of the fact that the coupling value required for criticality becomes arbitrarily small as a function of the curvature (the catalyzer). Hence, any finite value of the fermionic interactions ultimately becomes supercritical, typically driving the system towards the ordered phase.

We investigate this RG mechanism within the simple $3d$ Gross-Neveu model in the present work. We concentrate on two different curved backgrounds with constant negative curvature: a maximally symmetric space-time (Anti de Sitter) and a purely spatially curved case (Lobachevsky plane). For both cases, mean-field studies are already available, see [27] and [28, 33], respectively. Whereas the former allows for an analytic treatment in terms of simple functions, the latter is potentially relevant for curved layered condensed matter systems. For instance, the excitonic or anti-ferromagnetic instabilities in graphite and graphene have been associated with quantum phase transitions falling into the $3d$ Gross-Neveu universality class [38, 39]. As catalyzed symmetry breaking is manifestly driven by the long-range modes, the RG analysis allows us to estimate the required curvature in relation to the length scale of the sample.

This paper is organized as follows: in Sect. II, we briefly introduce the model and its formulation in curved space. Section III is devoted to an evaluation of the RG flow in its simplest formulation. The manifestation of gravitational catalysis is discussed in Sect. IV. We estimate the influence of finite probe length on gravitational catalysis in Sect. V by means of a pseudo-critical coupling. Conclusions are drawn in Sect. VI. Relevant technical details are deferred to the appendices.

II. GROSS-NEVEU MODEL IN CURVED SPACE

We aim at investigating the 3d Gross-Neveu model [40] in curved spacetime with metric $g_{\mu\nu}$ (Greek indices running from 0 to 2) and signature $(-, +, +)$ using functional RG methods. The microscopic action functional S at some ultraviolet (UV) scale Λ depends on the bare coupling constant $\bar{\lambda}_\Lambda$, the N Grassmann-valued fields $\psi = (\psi^i)$ and the N conjugated fields $\bar{\psi} = (\bar{\psi}^i)$,

$$\begin{aligned} S[\bar{\psi}^i, \psi^i] &= \int_x \left[\sum_{i=1}^N \bar{\psi}^i \not{\nabla} \psi^i + \frac{\bar{\lambda}_\Lambda}{2N} \left(\sum_{i=1}^N \bar{\psi}^i \psi^i \right)^2 \right] \\ &= \int_x \left[\bar{\psi} \not{\nabla} \psi + \frac{\bar{\lambda}_\Lambda}{2N} (\bar{\psi} \psi)^2 \right], \end{aligned} \quad (1)$$

where $\int_x = \int d^d x \sqrt{-g}$ is a shorthand for the integral over the d -dimensional spacetime and $g = \det g_{\mu\nu}$ is the determinant of the spacetime metric. The differential operator $\not{\nabla} = \gamma^\mu \nabla_\mu$ is composed from a set of d_γ -dimensional gamma matrices satisfying the Clifford algebra

$$\{\gamma_\mu, \gamma_\nu\} = 2g_{\mu\nu} \mathbf{I}, \quad (2)$$

where \mathbf{I} is the identity in spinor space. In the present work, we use the irreducible representation, such that $d_\gamma = 2$ specifies the dimension of the γ matrices as well as the number of Dirac components of the fermions. For our computations with fermions in curved space, we have actually used the Weldon formalism [41] which can be viewed as a generalization of the conventional vierbein formalism. However, a mapping to standard vierbein formulas is straightforward. The covariant derivative in the Weldon formalism reads

$$\nabla_\mu \psi^i = \partial_\mu \psi^i + \Gamma_\mu \psi^i, \quad (3)$$

accounting for covariance with respect to the spinor and spacetime structure. Here, Γ_μ is the affine spin connection, implicitly defined by

$$\begin{aligned} \text{(i)} \quad 0 &= \nabla_\mu \gamma^\nu = \partial_\mu \gamma^\nu + \Gamma_{\mu\rho}^\nu \gamma^\rho + [\Gamma_\mu, \gamma^\nu], \\ \text{(ii)} \quad 0 &= \text{tr } \Gamma_\mu, \end{aligned} \quad (4)$$

with $\Gamma_{\mu\rho}^\nu$ the Christoffel symbols.¹ In the present work, we are interested in a discrete “chiral” \mathbb{Z}_2 symmetry, where the nontrivial transformation is defined by [42]

$$\psi(x) \rightarrow -\psi(-x), \quad \bar{\psi}(x) \rightarrow \bar{\psi}(-x). \quad (5)$$

This symmetry acts simultaneously on all flavors. It can spontaneously be broken by a chiral condensate

¹ More generally, the spin connection Γ_μ can additionally accommodate a $U(1)$ gauge field \mathcal{A}_μ [41]. In this case, the right-hand side of (ii) in (4) would be given by $\text{tr } \Gamma_\mu = -id_\gamma q \mathcal{A}_\mu$, where q is the charge under the $U(1)$ gauge group. In the present work, we ignore such a $U(1)$ gauge sector, setting $\mathcal{A}_\mu = 0$.

$\langle \bar{\psi} \psi \rangle \neq 0$, which for finite interactions goes along with a mass gap generation. Incidentally, the 3d Gross-Neveu model actually has a much larger continuous $U(N)$ flavor symmetry also allowing for more complicated breaking patterns [43].²

III. FERMIONIC RG FLOWS IN CURVED SPACE

In the following, we use the functional renormalization group to compute the RG flow of the Gross-Neveu coupling as a function of the (negative) curvature. We employ the Wetterich equation [46], describing the flow of a scale-dependent effective action functional Γ_k as a function of an IR regulator scale k ,

$$\partial_k \Gamma_k[\bar{\psi}^i, \psi^i] = \frac{i}{2} \text{STr} \left[\left(\Gamma_k^{(2)} + R_k \right)^{-1} \partial_k R_k \right]. \quad (6)$$

The effective average action Γ_k is related to the standard generating functional for 1PI correlation functions in the limit $\Gamma = \Gamma_{k \rightarrow 0}$. Towards the UV cutoff $k \rightarrow \Lambda$, Γ_k approaches the microscopic action. The regularization is encoded in the regulator function R_k , see below. For reviews of the functional RG adapted to the present context, see Refs. [47–54].

In the present work, we evaluate the flow within a rather simple approximation for the effective action. For this, we truncate the effective action to

$$\Gamma_k[\bar{\psi}^i, \psi^i] = \int_x \left[\bar{\psi} \not{\nabla} \psi + \frac{\bar{\lambda}_k}{2N} (\bar{\psi} \psi)^2 \right], \quad (7)$$

where the only scale dependence lies in the four fermion coupling $\bar{\lambda}_k$. Furthermore, $\bar{\lambda}_k$ parametrically depends on the curvature of the background manifold. The IR regularization is ensured by a chirally symmetric regulator of the form

$$R_k(x, y) = \begin{pmatrix} \not{\nabla} r(\tau) & 0 \\ 0 & \not{\nabla}^T r(\tau^T) \end{pmatrix} \mathbb{1}(x, y), \quad (8)$$

$$\mathbb{1}(x, y) = \begin{pmatrix} \frac{\delta(x, y)}{\sqrt{-g}} & 0 \\ 0 & \frac{\delta(y, x)^T}{\sqrt{-g}} \end{pmatrix}, \quad \tau = -\frac{\not{\nabla}^2}{k^2}, \quad (9)$$

² In many 3d condensed matter systems where the Gross-Neveu model is considered as an effective theory, the low-energy degrees of freedom can be arranged into N_f 4-component Dirac spinors, corresponding to a reducible representation of the Dirac algebra. This reducible representation can be constructed from a suitable combination of 2-component spinors such that $N = 2N_f$ in terms of the counting of fermions of the present work, see, e.g., [44] for a review. Note that the Gross-Neveu interaction term considered in this work $\sim (\bar{\psi} \psi)^2$ corresponds to $\sim (\bar{\psi} \gamma_{45} \psi)^2$ in the reducible 4-component notation of [43] (or to $\sim (\bar{\psi} \gamma_{35} \psi)^2$ in the notation of [19, 33]) for even N . The critical properties of the discrete chiral transition are, however, identical to a 4-component Gross-Neveu model with a $(\bar{\psi} \psi)^2$ interaction as considered in [45].

where the superscript T denotes transposition in Dirac space, and $\delta(x, y)$ represents a spin-valued delta distribution, keeping track of the spinor or conjugate-spinor transformation properties associated with the spacetime arguments. In App. A, we briefly summarize our conventions.

For practical computations, we use a Callan-Symanzik type regulator, that facilitates the use of proper time representations,

$$r(x) = \sqrt{\frac{1+x}{x}} - 1. \quad (10)$$

Within our investigations we restrict ourselves to negative curvature, giving rise to gravitational catalysis. It is intuitively clear, that positive curvature (e.g., a sphere) generically suppresses IR modes and thus reduces the density of states of low lying modes [21, 22]. We also consider the system mainly in the large- N limit. At finite N , further pointlike fermionic self-interactions are generated which correspond to operators with an explicit curvature dependence.³ We expect no qualitative modifications from these operators and hence ignore them in the following. This approximation becomes exact in the limit $N \rightarrow \infty$.

It is straightforward (cf. App. A) to calculate the flow of the coupling as an implicit functional of the choice of the manifold, which enters via the spectrum of the Dirac operator

$$\partial_k \bar{\lambda}_k = -i \frac{2\bar{\lambda}_k^2}{\Omega N k^3} \text{STr} \left[(I + \tau)^{-2} \frac{\delta(x, y)}{\sqrt{-g}} \right]. \quad (11)$$

For this calculation, it suffices to project the flow onto constant fields $\psi^i(x) \equiv \Psi^i$, with $\partial_\mu \Psi^i = 0$. Here, $\Omega = \int_x 1$ denotes the spacetime volume. The operator occurring in the trace is related to the square of the regularized fermionic Green's function in curved spacetime. This has a direct correspondence to a Feynman diagram representation, see Fig. 1, as the flow in the present simple truncation is driven by a single fermion bubble (and RG-improved resummations thereof). In the following we distinguish between the cases of a maximally symmetric spacetime in Sect. III A which can be treated fully analytically, and a negatively curved space in Sect. III B, which is a more interesting case in view of two-dimensional condensed matter systems.

A. Maximally symmetric spacetime

The use of a Callan-Symanzik regulator shape function, cf. Eq. (10), facilitates to rewrite the right-hand

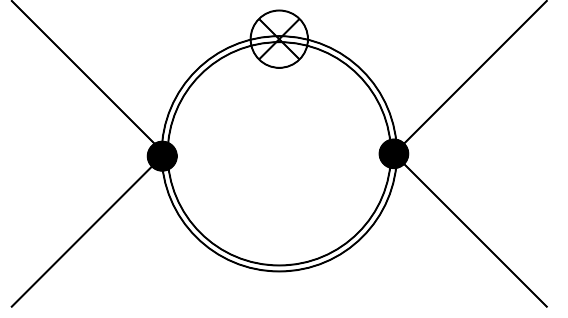


Figure 1. The diagram schematically exemplifies the fluctuation contributions to the flow of the Gross-Neveu coupling. The double lines represent the fermion propagator on the curved manifold. The full circles denote the RG-improved couplings, and the crossed circle marks the regulator insertion.

side of Eq. (11) in terms of a simple proper time representation. Other shape functions would still permit to use a proper time representation but would lead to more intricate k dependencies. The Laplace transform of the operator of (11) reads

$$(I + \tau)^{-2} \frac{\delta(x, y)}{\sqrt{-g}} = -k^4 \int_0^\infty ds s e^{-isk^2} e^{is\mathbb{V}^2} \frac{\delta(x, y)}{\sqrt{-g}}, \quad (12)$$

which upon insertion into (11) yields

$$\partial_k \bar{\lambda}_k = i \frac{2\bar{\lambda}_k^2 k}{\Omega N} \int_0^\infty ds s e^{-isk^2} \text{STr} \left[e^{is\mathbb{V}^2} \frac{\delta(x, y)}{\sqrt{-g}} \right]. \quad (13)$$

The expression inside the super trace is known as the heat kernel $K(x, y; s) = e^{is\mathbb{V}^2} \delta(x, y) / \sqrt{-g}$ of the (squared) Dirac operator. It satisfies

$$\begin{aligned} \text{(i)} \quad \partial_s K &= i\mathbb{V}^2 K, \\ \text{(ii)} \quad \lim_{s \searrow 0} K &= \frac{\delta(x, y)}{\sqrt{-g}}, \end{aligned} \quad (14)$$

and was calculated in [55] for any maximally symmetric space, with Euclidean signature. For our case the solution to this equation can be obtained in an easier way with a special ansatz (cf. App. B):

$$K = \frac{e^{i\frac{d_G^2}{4s}}}{\cosh w} \left(\frac{w}{s \sinh w} + i \frac{|R|}{12 \cosh w} \right) \frac{e^{-i\frac{\pi}{4}}}{(4\pi)^{\frac{3}{2}} \sqrt{s}} U, \quad (15)$$

where $w^2 = \frac{|R|d_G^2}{24}$, and $d_G(x, y)$ is the geodesic distance between the points x and y . The parallel transporter U (Wegner-Wilson line) is defined by

$$U(x, y) = \text{P exp} \left(- \int_0^1 dt \frac{dz^\mu(t)}{dt} \Gamma_\mu(z(t)) \right), \quad (16)$$

³ A similar mechanism has been observed in [19] for the case of a magnetic field, and the corresponding operators have been classified.

where P denotes the path ordering prescription and $z(t)$ is the geodesic between x and y with $z(t=0) = x$ and $z(t=1) = y$.

Now we are able to calculate the supertrace as

$$\text{STr} \left[e^{is\mathbb{V}^2} \frac{\delta(x,y)}{\sqrt{-g}} \right] = -\frac{2\Omega N}{(4\pi)^{\frac{3}{2}}\sqrt{s}} \left(\frac{1}{s} + i\frac{|R|}{12} \right) e^{-i\frac{\pi}{4}}, \quad (17)$$

and finally get

$$\partial_k \bar{\lambda}_k = -\frac{\bar{\lambda}_k^2}{2\pi} \left(1 + \frac{|R|}{24k^2} \right). \quad (18)$$

In terms of the dimensionless coupling,

$$\lambda_k = k\bar{\lambda}_k, \quad (19)$$

we obtain the beta function β_λ

$$\beta_\lambda = k\partial_k \lambda_k = \lambda_k - \frac{\lambda_k^2}{2\pi} \left(1 + \frac{|R|}{24k^2} \right). \quad (20)$$

This is an ordinary differential equation that parametrically depends on the curvature. It can be solved by straightforward integration:

$$\lambda_k = \frac{k}{\Lambda} \frac{\lambda_\Lambda}{1 - \frac{\lambda_\Lambda}{2\pi} \left(1 - \frac{k}{\Lambda} \right) \left(1 + \frac{|R|}{24k\Lambda} \right)}. \quad (21)$$

The initial value is given by the dimensionless coupling λ_Λ which in terms of the initial bare Gross-Neveu coupling reads $\lambda_\Lambda = \Lambda \bar{\lambda}_\Lambda$.

B. Negatively curved space

For the case of a manifold where the spatial part has a constant negative curvature, we choose a special set of coordinates such that the metric can be expressed as

$$(g_{\mu\nu}) = \begin{pmatrix} -1 & 0 & 0 \\ 0 & \hat{g}_{ij} \\ 0 & 0 & 0 \end{pmatrix}, \quad (22)$$

where \hat{g}_{ij} (Latin indices running from 1 to 2) represents the metric of a two dimensional maximally symmetric space and therefore only depends on the spatial coordinates. Hence the gamma matrices are time independent as well. The Christoffel symbols vanish for every time component $\Gamma_{\mu 0}^\rho = \Gamma_{\mu\nu}^0 = 0$ and also the curvature tensor vanishes if any index is zero $R_{\mu\nu\rho 0} = 0$. From Eq. (4) (i), we infer that the spin connection Γ_0 has to be proportional to I ,

$$0 = \nabla_0 \gamma^\nu = [\Gamma_0, \gamma^\nu]. \quad (23)$$

Moreover, From Eq. (4) (ii), we conclude that Γ_0 even has to vanish completely,

$$\text{tr} \Gamma_0 = 0. \quad (24)$$

This implies that the operator \mathbb{V}^2 is separable into

$$\begin{aligned} \mathbb{V}^2 \psi^i &= -\partial_0^2 \psi^i + \vec{\nabla}^2 \psi^i, \quad \vec{\nabla} \psi^i = \gamma^k \nabla_k \psi^i \\ &= -\partial_0^2 \psi^i + \vec{\nabla}^2 \psi^i - \frac{R}{4} \psi^i, \end{aligned} \quad (25)$$

where the curvature is only induced by the spatial components.

For a simpler calculation of the beta function, we perform a Wick rotation $x^0 \rightarrow -ix^0$ and perform again a Laplace transformation of the operator occurring in Eq. (11),

$$(I + \tau)^{-2} \frac{\delta(x,y)}{\sqrt{-g}} = k^4 \int_0^\infty ds \, se^{-sk^2} e^{s\mathbb{V}^2} \frac{\delta(x,y)}{\sqrt{-g}}. \quad (26)$$

We arrive at the Euclidean analogue of Eq. (13)

$$\partial_k \bar{\lambda}_k = \frac{2\bar{\lambda}_k^2 k}{\Omega N} \int_0^\infty ds \, se^{-sk^2} \text{STr} \left[e^{s\mathbb{V}^2} \frac{\delta(x,y)}{\sqrt{-g}} \right]. \quad (27)$$

Here, we calculate the super trace again with the aid of the heat kernel using that the differential operator \mathbb{V}^2 is separable and the delta distribution factorizes in a time like and a spatial part

$$e^{s\mathbb{V}^2} \frac{\delta(x,y)}{\sqrt{-g}} = e^{s\partial_0^2} \delta(x^0 - y^0) \cdot e^{s\vec{\nabla}^2} \frac{\delta(\vec{x}, \vec{y})}{\sqrt{\hat{g}}}, \quad (28)$$

where $\hat{g} = \det \hat{g}_{ij}$. The quantity \vec{x} denotes the spatial coordinates of x and should be treated as a set of coordinates and not as a vector. Both factors satisfy a heat-kernel equation and can be solved analytically, cf. [55],

$$e^{s\partial_0^2} \delta(x^0 - y^0) = \frac{e^{-\frac{(x^0 - y^0)^2}{4s}}}{\sqrt{4\pi s}}, \quad (29)$$

$$e^{s\vec{\nabla}^2} \frac{\delta(\vec{x}, \vec{y})}{\sqrt{\hat{g}}} = \frac{2 \cosh^{-1} \frac{\hat{w}}{2}}{(4\pi s)^{\frac{3}{2}} \sqrt{|R|}} \int_{\hat{w}}^\infty dv \frac{ve^{-\frac{v^2}{4s|R|}} \cosh \frac{v}{2}}{\sqrt{\cosh v - \cosh \hat{w}}} \hat{U}, \quad (30)$$

where $\hat{w}^2 = \frac{|R|\hat{d}_G^2}{2}$, \hat{U} is the parallel transporter for the spatial part and \hat{d}_G is the nonnegative spatial geodesic distance between \vec{x} and \vec{y} with $d_G^2(x,y) = \hat{d}_G^2(\vec{x}, \vec{y}) - (x^0 - y^0)^2$. Plugging these relations into Eq. (27) gives

$$\partial_k \bar{\lambda}_k = -\frac{\bar{\lambda}_k^2}{2\pi} \cdot \mathfrak{I}(\alpha_k), \quad \alpha_k = \sqrt{\frac{|R|}{2k^2}}, \quad (31)$$

$$\mathfrak{I}(\alpha) = \frac{\alpha}{2\pi} \int_0^\infty ds \int_0^\infty dv \frac{e^{-s - \frac{v^2}{4s}}}{s} v \coth \frac{\alpha v}{2}. \quad (32)$$

The s integral is an integral representation of the modified Bessel function of the second kind $K_0(v)$ [56]. Therefore, we have

$$\mathfrak{I}(\alpha) = \frac{\alpha}{\pi} \int_0^\infty dv \, v K_0(v) \coth \frac{\alpha v}{2}. \quad (33)$$

With these results we are again able to derive the beta function for the dimensionless coupling $\lambda_k = k\bar{\lambda}_k$,

$$\beta_\lambda = k\partial_k \lambda_k = \lambda_k - \frac{\lambda_k^2}{2\pi} \cdot \mathcal{I}(\alpha_k). \quad (34)$$

The integration of this ordinary differential equation depending parametrically on the curvature can be cast into an integral representation,

$$\lambda_k = \frac{k}{\Lambda} \frac{\lambda_\Lambda}{1 - \frac{\lambda_\Lambda}{2\pi} \alpha_\Lambda \int_{\alpha_\Lambda}^{\alpha_k} \frac{\mathcal{I}(\alpha)}{\alpha^2} d\alpha}, \quad \alpha_k = \sqrt{\frac{|R|}{2k^2}}. \quad (35)$$

This result is qualitatively similar to the maximally symmetric case of Eq. (21).

IV. GRAVITATIONAL CATALYSIS

Let us now analyze the consequences of the RG flows for the long-range properties of the Gross-Neveu model. For both background manifolds, β_λ considered as a function of λ_k is a parabola where the prefactor of the quadratic part is scale and curvature dependent, see Fig. 2. For vanishing curvature, the β_λ function vanishes at the two fixed points $\lambda_k = 0$ (Gaussian) and $\lambda_*(R=0) = \lambda_{cr} = 2\pi$ which corresponds to the well-known critical coupling of the Gross-Neveu model in flat space in this regularization scheme [45, 54]. This critical coupling separates the symmetric phase for $\lambda_\Lambda < \lambda_{cr}$ where the long range behavior is controlled by the non-interacting Gaussian fixed point from the chiral symmetry broken phase for $\lambda_\Lambda > \lambda_{cr}$. In the latter case, λ_k runs to large values towards the infrared. In the present simple truncation, λ_k in fact diverges at a finite scale k_{SB} signaling the transition into the ordered regime. The scale k_{SB} is thus characteristic for the physical scales in the ordered phase. In [57] it has been shown that k_{SB} actually agrees with the value of the dynamically generated fermion mass m_f as obtained in mean-field approximation. Since we are working in the large- N limit anyway, we will use this mean-field identification in the following: $m_f = k_{SB}$.

The existence of the non-Gaussian fixed point λ_{cr} can be attributed to the competition between the power-counting scaling (the linear coupling term in β_λ) and the interaction terms $\sim \lambda_k^2$. In our RG picture, the interaction terms are enhanced by negative curvature as soon as the wavelength of the fluctuations becomes of the order of the curvature scale. As a consequence, the interacting second zero of the β_λ function no longer is a true fixed point but becomes scale dependent. This “pseudo-critical coupling” $\lambda_p = \lambda_*(|R|/k^2)$ moves towards the Gaussian fixed point for decreasing scale k , see Fig. 2.

Any finite initial coupling strength λ_Λ will eventually become larger than $\lambda_*(|R|/k^2)$ for small RG scales $k \rightarrow 0$. By this mechanism, the system is forced into the symmetry-broken phase even at the weakest initial

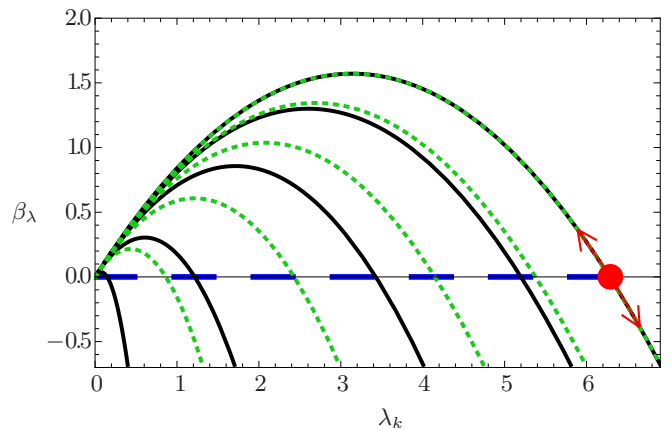


Figure 2. Plot of the RG β_λ function of the coupling λ_k for different values of the scale dependent negative curvature $\frac{|R|}{k^2}$ (from top to bottom: 0; 5; 20; 100; 1000). The black lines depict the β_λ functions for the maximally symmetric spacetime (AdS), cf. Eq. (20); arrows indicate the flow towards the IR. The green dotted graphs show the flows for the case of purely spatial curvature (Lobachevsky plane), cf. Eq. (34). In addition to the Gaussian fixed point, there exists a non Gaussian fixed point (full red circle at $\lambda_{cr} = 2\pi$ for the present regulator scheme), separating the symmetric phase for $\lambda_\Lambda < \lambda_{cr}$ from the broken phase for $\lambda_\Lambda > \lambda_{cr}$ for zero curvature. For finite curvature, this critical point becomes scale-dependent and moves towards the Gaussian fixed point for increasing scale dependent curvature, i.e., with decreasing IR scale for fixed curvature. In the case of vanishing curvature, the symmetry is preserved and no mass is generated for initial values λ_Λ in the blue dashed region.

coupling. We observe this mechanism in both cases of negative curvature, the maximally symmetric as well as the purely spatial curvature case. As we see in Fig. 2 the influence of the curvature is somewhat stronger in the maximally symmetric case.

As discussed above, we calculate the symmetry breaking scale k_{SB} by searching for a zero of the inverse coupling. The fermion mass m_f corresponding to this scale where the RG flow enters the symmetry-broken regime can thus be computed from the criterion

$$\lambda_{k=m_f}^{-1}(|R|/m_f^2) = 0. \quad (36)$$

Upon partial bosonization (Hubbard-Stratonovich transformation), λ_k^{-1} is related to the mass parameter of a composite bosonic field. Hence the divergence of the fermionic self-interaction simply corresponds to onset of the order parameter [54, 58, 59]. Let us now analyze the two different backgrounds under consideration in detail.

A. Maximally symmetric spacetime

In the maximally symmetric case, the fermion mass defined by the criterion Eq. (36) can be straightforwardly

computed from the running coupling Eq. (21), yielding

$$\frac{m_f}{\Lambda} = \frac{1}{2} - \frac{|R|}{48\Lambda^2} - \frac{\pi}{\lambda_\Lambda} + \sqrt{\left(\frac{1}{2} - \frac{|R|}{48\Lambda^2} - \frac{\pi}{\lambda_\Lambda}\right)^2 + \frac{|R|}{24\Lambda^2}}. \quad (37)$$

Plots of this gravitationally catalyzed fermion mass are shown as a function of the curvature as solid lines in Fig. 3. Let us discuss this result in various limits. In the zero-curvature limit $R = 0$, we find $m_f = 0$ for $\lambda_\Lambda \leq 2\pi$. For super-critical couplings $\lambda_\Lambda > 2\pi$, we rediscover the standard mean-field result in $3d$,

$$m_{f,0} \equiv m_f(R=0) = \Lambda \left(1 - \frac{2\pi}{\lambda_\Lambda}\right). \quad (38)$$

This is in perfect agreement with the known behavior in flat spacetime.

Provided the fermion system is initially weakly coupled, $\lambda_\Lambda \ll \lambda_{\text{cr}} = 2\pi$, a leading order expansion can be performed for any value of the curvature, resulting in

$$m_f \simeq \frac{\Lambda}{1 + \frac{48\pi\Lambda}{|R|\bar{\lambda}_\Lambda}}, \quad \text{for } \bar{\lambda}_\Lambda \Lambda \ll 1, \quad (39)$$

where we have reinserted the dimensionful initial coupling $\bar{\lambda}_\Lambda = \lambda_\Lambda/\Lambda$. If we additionally consider the limit of small curvature, we find a linear dependence of the fermion mass on both the curvature as well as the coupling,

$$m_f \simeq \frac{1}{48\pi} |R| \bar{\lambda}_\Lambda. \quad (40)$$

By contrast, in the limit of large curvature, $|R|/(48\pi\Lambda^2) \gg \pi/\lambda_\Lambda \gg 1$, we find that $m_f \rightarrow \Lambda$. In other words, large curvature induces immediate chiral symmetry breaking, such that the induced mass becomes of the order of the cutoff. Incidentally, this result is similar for the large-coupling limit: for $\lambda_\Lambda \gg 2\pi$, we again find that $m_f \rightarrow \Lambda$ to leading order independently of the curvature.

The above results display explicit UV cutoff and regularization-scheme dependencies. Since the $3d$ Gross-Neveu model is asymptotically safe and thus non-perturbatively renormalizable [19], we can remove the UV cutoff by keeping an IR observable fixed while sending $\Lambda \rightarrow \infty$. This “line of constant physics” defines a renormalized trajectory. This can most conveniently be done in the super-critical regime where $\lambda_\Lambda > 2\pi$ such that the fermion mass in flat-space $m_{f,0}$ of Eq. (38) defines a natural IR renormalization point.⁴ In this case,

⁴ In the sub-critical regime, the model is quasi conformal and can be renormalized, e.g., by fixing the coupling λ_k at a suitable renormalization point $k = \mu$ to a specific value.

the generated fermion mass in the limit $\Lambda \rightarrow \infty$ can be written as

$$\begin{aligned} \frac{m_f}{m_{f,0}} &= \frac{1}{2} + \sqrt{\frac{1}{4} + \frac{|R|}{24m_{f,0}^2}} \\ &\simeq 1 + \frac{|R|}{24m_{f,0}^2}, \end{aligned} \quad (41)$$

where the first line holds for arbitrary curvature, and the second line represents a weak-curvature expansion being in perfect agreement with [27].

We emphasize that the fermions acquire a mass $m_f > 0$ for any given λ_Λ as long as the curvature is nonvanishing. While we expect the tendency to drive the fermion system towards the broken phase through gravitational catalysis to remain also beyond our truncation, fluctuations of bosonic composites entering beyond the large- N limit typically provide for an opposite tendency. Hence, the status of gravitational catalysis beyond mean-field remains an interesting question. Analogously, the effects of beyond-mean-field fluctuations on magnetic catalysis are under active current investigation [20, 60].

B. Negatively curved space

In the case of pure spatial curvature, the criterion Eq. (36) cannot be resolved analytically, but we can give an implicit equation for the induced fermion mass m_f

$$0 = \frac{2\pi}{\lambda_\Lambda} - \alpha_\Lambda \int_{\alpha_\Lambda}^{\alpha_{m_f}} \frac{\mathfrak{I}(\alpha)}{\alpha^2} d\alpha, \quad \alpha_k = \sqrt{\frac{|R|}{2k^2}}, \quad (42)$$

which can be solved numerically. Though the basic picture does not differ much from the maximally symmetric case, there are some interesting differences. As can already be inferred from the beta function in Fig. 2 (dotted lines), the curvature induced mass in the spatially curved case is smaller than in the maximally symmetric case, cf. Fig. 3. Several limits can be discussed in an analytic fashion, using the series representation of $\mathfrak{I}(\alpha)$ developed in App. C. Furthermore, we need the integral $\mathfrak{F}(\alpha)$ defined by

$$\begin{aligned} \text{(i)} \quad \mathfrak{F}(\alpha) &= \int \frac{\mathfrak{I}(\alpha)}{\alpha^2} d\alpha, \\ \text{(ii)} \quad \lim_{\alpha \rightarrow \infty} \left(\mathfrak{F}(\alpha) - \frac{\ln \alpha}{\pi} \right) &= 0, \end{aligned} \quad (43)$$

where (ii) fixes the constant of integration. The explicit calculation is done in App. C. The defining equation for the fermion mass in terms of \mathfrak{F} is

$$\mathfrak{F}(\alpha_{m_f}) = \mathfrak{F}(\alpha_\Lambda) + \frac{2\pi}{\lambda_\Lambda \alpha_\Lambda}. \quad (44)$$

This representation provides us with some interesting insight. First, we can show that there exists a unique

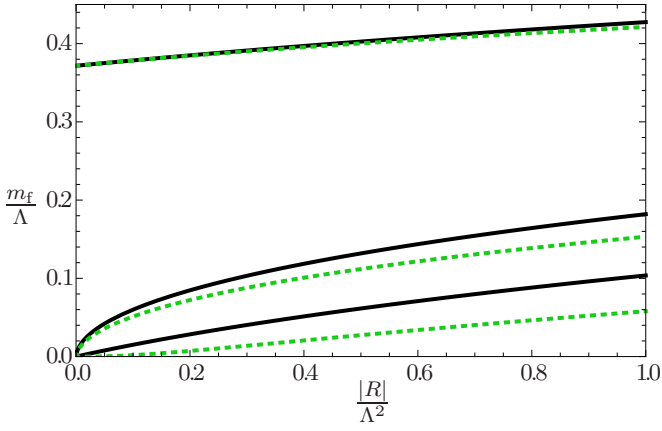


Figure 3. Gravitationally catalyzed fermion masses (mean-field level) as a function of negative curvature in units of the UV cutoff. The solid black lines display the maximally symmetric case, whereas the purely spatially curved case is shown as green dotted lines. The sets of three different lines correspond to super-critical, critical, and sub-critical bare fermion couplings, $\lambda_\Lambda \simeq 1.6\lambda_{\text{cr}}, \lambda_{\text{cr}}, 0.8\lambda_{\text{cr}}$ from top to bottom ($\lambda_{\text{cr}} = 2\pi$). As long as the background manifold is negatively curved, $|R| > 0$, a finite fermion mass is generated.

solution to this equation with $0 < m_f < \Lambda$ for any given negative curvature $|R| > 0$ and $\lambda_\Lambda > 0$. This can be seen in two steps. The uniqueness is because the function $\mathfrak{F}(\alpha) \in (-\infty, \infty)$ for $\alpha \in (0, \infty)$ is bijective. This property holds, because $\mathfrak{I}(\alpha)$ is positive and therefore \mathfrak{F} is strictly monotonically increasing. Owing to $\mathfrak{I}(\alpha)/\alpha^2 \rightarrow 1/\alpha^2$ for small $\alpha \rightarrow 0$ and $\mathfrak{I}(\alpha)/\alpha^2 \rightarrow 1/(\pi\alpha)$ for large $\alpha \rightarrow \infty$, the function \mathfrak{F} is not bounded. Since by assumption $2\pi/(\lambda_\Lambda\alpha_\Lambda) > 0$, it follows from Eq. (44) that $\mathfrak{F}(\alpha_{m_f}) > \mathfrak{F}(\alpha_\Lambda)$ has to hold, which implies that $\alpha_{m_f} > \alpha_\Lambda$ because of the monotonic behavior. This demonstrates that $0 < m_f < \Lambda$ as claimed above.

Let us first check the flat spacetime limit $|R| \rightarrow 0$. In complete agreement with Eq. (38), we find again that

$$\frac{2\pi}{\lambda_\Lambda} = \lim_{|R| \rightarrow 0} [\alpha_\Lambda \mathfrak{F}(\alpha_{m_f}) - \alpha_\Lambda \mathfrak{F}(\alpha_\Lambda)] = 1 - \frac{m_{f,0}}{\Lambda}, \quad (45)$$

where we have used Eq. (C9).

In the weak coupling regime, we expect the fermion mass to be small compared to the curvature scale, cf. Eq. (40). Hence, we need $\mathfrak{F}(\alpha)$ for large argument as provided by Eq. (C10),

$$\mathfrak{F}(\alpha \gg 1) \simeq \frac{\ln \alpha}{\pi}. \quad (46)$$

Using this asymptotic behavior for $\mathfrak{F}(\alpha_{m_f})$, we infer from Eq. (44) that

$$m_f \simeq \sqrt{\frac{|R|}{2}} \exp \left[-\frac{\pi}{\alpha_\Lambda} \left(\frac{2\pi}{\lambda_\Lambda} + \alpha_\Lambda \mathfrak{F}(\alpha_\Lambda) \right) \right], \quad \alpha_\Lambda = \sqrt{\frac{|R|}{2\Lambda^2}}. \quad (47)$$

If in addition, the curvature is small, i.e., $\alpha_\Lambda \ll 1$, we can use the corresponding expansion of Eq. (C9) and replace $\alpha_\Lambda \mathfrak{F}(\alpha_\Lambda) \rightarrow -1$. Taking differences arising from the Dirac representation into account, the exponential inverse-coupling dependence is in perfect agreement with the results of [33].

Despite the overall similarities to the maximally symmetric case, we observe that the weak-coupling and weak-curvature limit of the case with pure spatial curvature shows some distinct differences. In particular, there is an exponential non-analytic dependence of the fermion mass on the coupling as well as on the curvature.

This difference is reminiscent to magnetic catalysis in $d = 2 + 1$ and $d = 3 + 1$ [2], where the fermion gap is analytic in $d = 2 + 1$, but shows an essential singularity in the coupling in $d = 3 + 1$. Also in the present case, such a singularity shows up similar to BCS gap formation, as a consequence of the effective dimensional reduction of the fermionic fluctuation spectrum to $d \rightarrow 1 + 1$ [36]. Also in this respect, our functional RG picture is in perfect agreement with previous studies [33, 37].

V. PSEUDO-CRITICAL COUPLING AND PROBE SIZE

At zero curvature, the 3d Gross-Neveu model exhibits a critical coupling strength corresponding to a quantum critical point above which chiral symmetry is broken at large length scales. This critical coupling manifests itself as a non-Gaussian fixed point of the RG flow. In the present regularization scheme, we identified $\bar{\lambda}_{\text{cr}} = 2\pi/\Lambda$, or $\lambda_{\text{cr}} = 2\pi$ in dimensionless conventions. As illustrated in Fig. 2, the fixed point strictly speaking no longer exists at finite negative curvature. The nontrivial zero of the β_λ function becomes scale dependent and eventually merges with the Gaussian fixed point in the deep IR for $k \rightarrow 0$, such that only the chirally broken branch of the β_λ function remains.

Let us call the nontrivial zero of β_λ a pseudo-critical coupling λ_p . We find

$$\lambda_p = \frac{\lambda_{\text{cr}}}{1 + \frac{|R|}{24k^2}} \quad (48)$$

for the maximally symmetric case, cf. Eq. (20), and

$$\lambda_p = \frac{\lambda_{\text{cr}}}{\mathfrak{I}\left(\sqrt{\frac{|R|}{2k^2}}\right)} \quad (49)$$

for the spatially curved case, cf. Eq. (34). Since $\lambda_p = \lambda_p(k)$ is a monotonically decreasing function of scale k , the coupling λ_k can eventually exceed λ_p such that the system becomes critical and runs towards the ordered phase. In this sense,

$$\lambda_{k_c} = \lambda_p(k_c) \quad (50)$$

can be viewed as a criticality condition [61], defining a scale k_c , where the system becomes critical. For lower scale, the system is driven towards the symmetry broken regime which is ultimately entered at $k_{\text{SB}} < k_c$ defined above. The value of k_c depends on the curvature as well as the initial coupling λ_Λ (the latter is considered as initially subcritical here and in the following).

The preceding discussion implicitly assumed that k can run over all scales down to $k = 0$, such that the criticality condition (50) can eventually always be satisfied. However, if, for instance, the system has a finite volume characterized by a finite length scale L , also the fluctuation momenta are restricted, typically leading to an IR cut-off $k_L = \pi/L$.⁵ One may think of a finite probe length, such as, e.g., the size of a layer of graphene. This finite probe length L can lead to a screening of the gravitationally catalyzed ordered regime if k_L is larger than the would-be critical scale k_c . Hence, $\lambda_p(k_L)$ can be viewed as a lower bound for the coupling strength required for symmetry breaking in a real system of finite length. It thus generalizes the critical coupling at infinite volume and zero curvature to the situation of finite volume and finite curvature.

It is instructive to study λ_p as a function of the length scale L measured in units of a typical curvature length scale which we define by $r = 1/\sqrt{|R|}$. For finite systems, this gives an estimate for how strongly a probe has to be curved in order to exhibit gravitational catalysis. In turn, for a given curvature of the probe, λ_p provides an estimate for the initial coupling strength required for symmetry breaking in the finite system. For instance, for the maximally symmetric case, we read off from Eq. (48) that

$$\lambda_p(k_L = \pi/L) = \frac{\lambda_{\text{cr}}}{1 + \frac{L^2}{24\pi^2 r^2}}. \quad (51)$$

For the spatially curved case, we incidentally find the same result in the limit of small curvature, i.e., $L/r \ll 1$, using the expansion (C3) which is accurate even for values of $L/r \simeq \mathcal{O}(1)$. By contrast, the large curvature limit for the spatially curved case is different, cf. Eq. (C7):

$$\lambda_p(k_L = \pi/L) = \sqrt{2}\pi^2 \frac{r}{L} \lambda_{\text{cr}}, \quad \frac{r}{L} \ll 1. \quad (52)$$

From Eq. (51), it is obvious that probe length to curvature ratios up to $L/r \simeq \mathcal{O}(1)$ lead to pseudo-critical couplings λ_p which deviate from the zero-curvature critical coupling of the Gross-Neveu model only below the 1% level. Significant deviations only occur for L being an order of magnitude larger than the curvature scale r . From the viewpoint of curvature-deformed condensed matter systems, a ratio of $L/r \simeq \mathcal{O}(1)$ appears to be “large” in the sense that – loosely speaking – a spatially

curved $2d$ planar probe embedded in $3d$ Euclidean space would rather look like a $3d$ object.

Another way to interpret these results is the following: consider a finite-probe system with a subcritical bare coupling, $\lambda_\Lambda < \lambda_{\text{cr}}$, thus being in the symmetric (e.g. semimetal) phase. In order to gravitationally catalyze a transition to a broken (gapped or insulating) phase, the criticality condition (50) has to be met for a sufficiently large $k_c > k_L$. In view of Eq. (51) this requires comparatively strong curvature, i.e., a small curvature length scale r compared with the probe length L .

VI. CONCLUSION AND OUTLOOK

We have investigated the phenomenon of gravitational catalysis in the $3d$ Gross-Neveu model on specific manifolds with constant negative curvature. While the mechanism had already been studied frequently with mean-field methods as well as from the viewpoint of the fluctuation spectrum of the Dirac operator, we have added a new renormalization group picture to the comprehensive understanding of this phenomenon. The essence of this picture is that the critical coupling of the fermionic system, corresponding to a quantum phase transition in flat spacetime, is transmuted into a scale-dependent pseudo-critical coupling that flows to zero as a consequence of long-wavelength fluctuations (compared to the curvature scale). In this manner, the infinite-volume fermion system becomes critical for any arbitrarily weak coupling.

We have identified the RG (pseudo-) fixed point mechanism for two example manifolds of constant negative curvature: a maximally symmetric spacetime (Anti de Sitter) and a purely spatially curved case (Lobachevsky plane). Both manifolds support the mechanism of gravitational catalysis, but exhibit a rather different behavior as far as the dependence of chiral symmetry breaking on the coupling and the curvature are concerned. The maximally symmetric case shows a linear dependence (to leading order) on both quantities which makes clear that the phenomenon is essentially perturbative, being reminiscent of the “quantum anomaly” for fermions in a magnetic field [62]. By contrast, order parameters indicating the symmetry broken state such as the induced fermion mass exhibit an essential singularity in both the coupling and the curvature for the case of the purely spatially curved case. This is in many respects similar to BCS-type gap formation. Again, our renormalization group picture goes hand in hand here with properties of the fermionic fluctuation spectrum, as analyzed in [36].

As a benefit, the functional renormalization group also gives a simple access to systems of finite extent by identifying the RG infrared cutoff with an inverse length scale. In this manner, we can estimate the fate of gravitational catalysis in finite systems. In fact, the phenomenon only occurs, as long as the curvature radius is sufficiently small compared to the systems length scale. We have been able to phrase this statement quantitatively by introducing a

⁵ Here, we tacitly assume that the boundary conditions are such that zero modes do not occur.

pseudo-critical coupling. Thinking in terms of curved layered condensed matter systems, rather large curvatures are needed compared to a realizable probe length in order to drive a sub-critical system into a phase dominated by gravitational catalysis.

We would like to emphasize that an immediate application of our results to condensed matter systems would only be possible for reparametrization invariant systems such as fluid membranes [63], curvature effects of which can be mapped onto the language of Riemannian geometry. For tethered membranes or general lattice systems, further phenomena connected to extrinsic curvature or curvature related defects can become relevant. In this context, it is interesting to note that an external strain exerted on a graphene sheet in flat space induces a pseudo-magnetic field [64], that may also support (pseudo-)magnetic catalysis. For such systems, we hence expect an interesting interplay between these various effects if we expose them to negative curvature inducing strain.

Finally, gravitational catalysis may become relevant in the context of asymptotically safe quantum gravity [65]. In conjunction with fermionic degrees of freedom [66], the UV fixed point determining the shape of the universe at highest energies might go along with a negative (though scale-dependent) curvature [67]. Whether or not gravitational catalysis in connection with gravitationally modified critical fermion interactions [68] could become active and impose constraints on the matter content of the universe then is a highly involved question that deserves to be investigated in greater depth.

ACKNOWLEDGMENTS

The authors thank Astrid Eichhorn, Lukas Janssen, Daniel Scherer, René Sondenheimer, and Andreas Wipf for valuable discussions and acknowledge support by the DFG under grants Gi 328/5-2 (Heisenberg program), GRK1523 and FOR 723.

Appendix A: Derivation of the beta function

Let us first introduce our conventions. In the Weldon formalism [41], the Dirac conjugate spinor $\bar{\psi}$ is related to the hermitean conjugate of the spinor ψ via the spin metric h

$$\bar{\psi} = \psi^\dagger h, \quad (\text{A1})$$

which is implicitly defined by

$$\begin{aligned} \text{(i)} \quad & h^\dagger = -h, \\ \text{(ii)} \quad & \gamma_\mu^\dagger = -h\gamma_\mu h^{-1}, \\ \text{(iii)} \quad & \nabla_\mu h = \partial_\mu h - h\Gamma_\mu - \Gamma_\mu^\dagger h = 0. \end{aligned} \quad (\text{A2})$$

This gives rise to the following properties of the building blocks of the Gross-Neveu action:

$$\begin{aligned} \text{(i)} \quad & \nabla_\mu \bar{\psi} = \partial_\mu \bar{\psi} - \bar{\psi}\Gamma_\mu, \\ \text{(ii)} \quad & (\bar{\psi}\psi)^* = \bar{\psi}\psi, \\ \text{(iii)} \quad & \int_x (\bar{\psi}\nabla\psi)^* = \int_x \bar{\psi}\nabla\psi. \end{aligned} \quad (\text{A3})$$

Choosing the spin metric h to be anti-hermitean in Eq. (A2) (i) is convenient for our metric and Clifford algebra conventions, but differs from [41]. Also, the absence of any imaginary factor of “i” in the fermion kinetic term is due to these conventions.

The flow equation (6) uses a rather condensed notation. More concretely, we work in field space parameterized by the collective fields

$$\phi = \begin{pmatrix} \psi \\ \bar{\psi}^\text{T} \end{pmatrix}, \quad \bar{\phi} = \begin{pmatrix} \bar{\psi} \\ \psi^\text{T} \end{pmatrix}, \quad (\text{A4})$$

representing Grassmann-valued functions on the manifold, reminiscent to Nambu-Gorkov spinors. For instance, the classical action amended by the regulator term which is used for deriving the flow equation from the functional integral (cf. [47–54]), reads in these conventions

$$S_k[\phi] = S[\phi] + \frac{1}{2} \int_x \int_y \bar{\phi}(x) R_k(x, y) \phi(y). \quad (\text{A5})$$

These conventions differ slightly from those commonly used, see, e.g., [59], but turn out to be advantageous for coordinate space computations on curved manifolds. For instance, the representation of the unit element in field space becomes rather intuitive,

$$\mathbb{1}(x, y) = \phi(x) \frac{\overleftarrow{\delta}}{\delta\phi(y)} = \frac{\overrightarrow{\delta}}{\delta\bar{\phi}(x)} \phi(y) = \begin{pmatrix} \frac{\delta(x, y)}{\sqrt{-g}} & 0 \\ 0 & \frac{\delta(y, x)^\text{T}}{\sqrt{-g}} \end{pmatrix}. \quad (\text{A6})$$

By $\delta(x, y)$, we denote the spin-valued delta distribution, which fulfills

$$\begin{aligned} \text{(i)} \quad & \psi(x) = \int_y \frac{\delta(x, y)}{\sqrt{-g}} \psi(y), \\ \text{(ii)} \quad & \bar{\psi}(x) = \int_y \bar{\psi}(y) \frac{\delta(y, x)}{\sqrt{-g}}. \end{aligned} \quad (\text{A7})$$

Therefore,

$$\nabla_\mu^{(x)} \frac{\delta(x, y)}{\sqrt{-g}} = \partial_\mu^{(x)} \frac{\delta(x, y)}{\sqrt{-g}} + \Gamma_\mu \frac{\delta(x, y)}{\sqrt{-g}} \quad (\text{A8})$$

has to hold. With this notation, we indicate that $\delta(x, y)$ transforms as a spinor in x and a Dirac-conjugated spinor in y , i.e. $\delta(x, y)$ can be interpreted as $\delta(x, y) = \delta(x - y)U(x, y)$, with the standard scalar delta distribution $\delta(x - y)$. We remark that there is a difference be-

tween $\delta(x, y)$ and $\delta(y, x)^T$ in the spinor structure, since

$$\nabla_\mu^{T(x)} \frac{\delta(y, x)^T}{\sqrt{-g}} = \partial_\mu^{(x)} \frac{\delta(y, x)^T}{\sqrt{-g}} - \Gamma_\mu^T \frac{\delta(y, x)^T}{\sqrt{-g}} \quad (\text{A9})$$

$$= \left(\nabla_\mu^{(x)} \frac{\delta(y, x)}{\sqrt{-g}} \right)^T. \quad (\text{A10})$$

For the evaluation of the flow equation Eq. (6), we proceed in a standard fashion. We decompose

$$\Gamma_k^{(2)} + R_k = \mathcal{F}_k + \mathcal{P}_k \quad (\text{A11})$$

into a field-dependent part \mathcal{F}_k and a field-independent part \mathcal{P}_k in order to expand the Wetterich equation in powers of the fields,

$$\partial_k \Gamma_k = \frac{i}{2} \sum_{n=0}^{\infty} (-1)^n \text{STr} [(\mathcal{P}_k^{-1} \partial_k R_k)(\mathcal{P}_k^{-1} \mathcal{F}_k)^n]. \quad (\text{A12})$$

Since

$$\mathcal{F}_k = -\frac{\bar{\lambda}_k}{N} \begin{pmatrix} -[(\bar{\Psi}\Psi)\text{I} + \Psi\bar{\Psi}] & \Psi\Psi^T \\ \bar{\Psi}^T\Psi & [(\bar{\Psi}\Psi)\text{I} + \Psi\bar{\Psi}]^T \end{pmatrix} \mathbb{1}, \quad (\text{A13})$$

$$\mathcal{P}_k = i k \begin{pmatrix} \sqrt{\tau}(\text{I} + r(\tau)) & 0 \\ 0 & \sqrt{\tau^T}(\text{I} + r(\tau^T)) \end{pmatrix} \mathbb{1}, \quad (\text{A14})$$

we observe that only the term $n = 2$ in Eq. (A12) can contribute to the flow of $\bar{\lambda}_k$. We need

$$\mathcal{P}_k^{-1} \partial_k R_k = \frac{2}{k} \begin{pmatrix} \frac{\tau r'(\tau)}{\text{I} + r(\tau)} & 0 \\ 0 & \frac{\tau^T r'(\tau^T)}{\text{I} + r(\tau^T)} \end{pmatrix} \mathbb{1} \quad (\text{A15})$$

with $r'(x) = \frac{d}{dx} r(x)$, and therefore only the diagonal of $(\mathcal{P}_k^{-1} \mathcal{F}_k)^2$ is required. In the limit $N \rightarrow \infty$, only the following terms remain:

$$[(\mathcal{P}_k^{-1} \mathcal{F}_k)^2]_{11}(x, y) = -\frac{\bar{\lambda}_k^2}{N^2 k^2} \frac{(\bar{\Psi}\Psi)^2}{\tau(\text{I} + r(\tau))^2} \frac{\delta(x, y)}{\sqrt{-g}}, \quad (\text{A16})$$

$$[(\mathcal{P}_k^{-1} \mathcal{F}_k)^2]_{22}(x, y) = [(\mathcal{P}_k^{-1} \mathcal{F}_k)^2]_{11}^T(y, x). \quad (\text{A17})$$

The LHS of Eq. (A12) boils down to

$$\partial_k \Gamma_k = \frac{\partial_k \bar{\lambda}_k}{2N} (\bar{\Psi}\Psi)^2 \Omega, \quad (\text{A18})$$

and the RHS yields

$$\begin{aligned} & \frac{i}{2} \text{STr} [(\mathcal{P}_k^{-1} \partial_k R_k)(\mathcal{P}_k^{-1} \mathcal{F}_k)^2] \\ &= i \frac{2\bar{\lambda}_k^2}{N^2 k^3} (\bar{\Psi}\Psi)^2 \text{STr} \left[\frac{r'(\tau)}{(\text{I} + r(\tau))^3} \frac{\delta(x, y)}{\sqrt{-g}} \right]. \end{aligned} \quad (\text{A19})$$

Inserting the Callan-Symanzik regulator (10), we end up with Eq. (11) of the main text.

Appendix B: Derivation of the heat kernel

Following [55], we choose for the heat kernel satisfying Eq. (14) the ansatz

$$K(x, y; s) = f(d_G(x, y), s) \cdot U(x, y) \quad (\text{B1})$$

where f is a scalar function of d_G the geodesic distance and the proper time s . Plugging this into equation (14) using $A = \sqrt{\frac{|R|}{6}} \coth(2w)$, $B = \sqrt{\frac{|R|}{96}} \tanh w$ and

$$\begin{aligned} \text{(i)} \quad & n_\mu n^\mu = 1, \quad n_\mu = \partial_\mu d_G, \\ \text{(ii)} \quad & \partial_\mu n_\nu - \Gamma_{\mu\nu}^\rho n_\rho = A(g_{\mu\nu} - n_\mu n_\nu), \\ \text{(iii)} \quad & \nabla_\mu U = B[\gamma_\mu, \gamma_\nu] n^\nu U, \end{aligned} \quad (\text{B2})$$

cf. [55], we get

$$0 = \left(\frac{|R|}{4} - 8B^2 \right) f + 2A f' + f'' + i f \quad (\text{B3})$$

with $f' = \partial_{d_G} f$, $\dot{f} = \partial_s f$. Because of the boundary condition for K and the regularity of $U(x, y = x) = \text{I}$ we observe that

$$\lim_{s \searrow 0} f = \frac{\delta(x - y)}{\sqrt{-g}}, \quad (\text{B4})$$

has to hold, with $\delta(x - y)$ representing the standard delta distribution. One suitable representation for the delta distribution in $3d$ maximally symmetric space with negative curvature in the limit $s \searrow 0$ is

$$\frac{\delta(x - y)}{\sqrt{-g}} = \frac{e^{-i\frac{\pi}{4}}}{(4\pi s)^{\frac{3}{2}}} \exp\left(i \frac{d_G^2}{4s}\right). \quad (\text{B5})$$

Next, we factorize f into the delta part and an auxiliary function p of d_G and s ,

$$f(d_G, s) = \frac{p(d_G, s)}{\sqrt{s}} \frac{e^{-i\frac{\pi}{4}}}{(4\pi)^{\frac{3}{2}}} \exp\left(i \frac{d_G^2}{4s}\right). \quad (\text{B6})$$

Expanding p in powers of $\frac{1}{s}$ and using the boundary conditions,

$$p = \frac{1}{s} p_1(d_G) + i p_0(d_G), \quad (\text{B7})$$

leads to

$$\begin{aligned} \text{(i)} \quad & 0 = -\left(\frac{1}{d_G} - A\right) p_1 + p_1', \\ \text{(ii)} \quad & 0 = d_G A p_0 + d_G p_0' + \left(8B^2 - \frac{|R|}{4}\right) p_1 - 2A p_1' - p_1'', \\ \text{(iii)} \quad & 0 = \left(8B^2 - \frac{|R|}{4}\right) p_0 - 2A p_0' - p_0'', \end{aligned} \quad (\text{B8})$$

with the boundary condition $p_1(0) = 1$. From equation (i) and the boundary condition, we see

$$p_1 = \frac{2w}{\sinh(2w)}. \quad (\text{B9})$$

Plugging this into (ii) gives

$$p_0 = \frac{|R|}{12 \cosh^2 w}, \quad (\text{B10})$$

where we have eliminated the constant of integration using equation (iii). From this, we finally get

$$K = \frac{e^{i\frac{d_G^2}{4s}}}{\cosh w} \left(\frac{w}{s \sinh w} + i \frac{|R|}{12 \cosh w} \right) \frac{e^{-i\frac{\pi}{4}}}{(4\pi)^{\frac{3}{2}} \sqrt{s}} U. \quad (\text{B11})$$

Appendix C: Curvature expansion

For the detailed analysis of the spatially curved case, the integral representation of the running coupling Eq. (35) can be studied in various limits analytically. More specifically, $\mathfrak{I}(\alpha)$ as defined in Eq. (33) can be expanded for small and for large values of α . Let us first consider an expansion of this function about $\alpha = 0$, starting with an expansion of the integrand,

$$\alpha v \coth \frac{\alpha v}{2} \simeq 2 + \frac{1}{6}(\alpha v)^2 - \frac{1}{360}(\alpha v)^4 + \mathcal{O}((\alpha v)^6). \quad (\text{C1})$$

Using the standard integral

$$\int_0^\infty dv v^{2k} K_0(v) = 2^{2k-1} \Gamma\left(\frac{2k+1}{2}\right)^2 = \frac{\pi}{2^{2k+1}} \left(\frac{(2k)!}{k!}\right)^2, \quad (\text{C2})$$

the small α expansion of $\mathfrak{I}(\alpha)$ can be computed to any order. To order α^4 , we find

$$\mathfrak{I}(\alpha) \simeq 1 + \frac{\alpha^2}{12} - \frac{\alpha^4}{80}. \quad (\text{C3})$$

Due to the factorial growth of the coefficients, cf. Eq. (C2), the expansion is an asymptotic series. By comparison with the numerical result, the accuracy of Eq. (C3) turns out to be above 99% up to $\alpha \simeq 1$.

A similar approximation can be done for large α by expanding

$$\coth \frac{\alpha v}{2} = \frac{1 + e^{-\alpha v}}{1 - e^{-\alpha v}} = 1 + 2 \sum_{n=1}^{\infty} e^{-n\alpha v}, \quad (\text{C4})$$

which holds for any $\alpha v > 0$. Next, we employ

$$\int_0^\infty dv v K_0(v) e^{-n\alpha v} = \frac{-1}{(n\alpha)^2 - 1} + \frac{n\alpha \operatorname{arcosh}(n\alpha)}{((n\alpha)^2 - 1)^{\frac{3}{2}}}, \quad (\text{C5})$$

which can be used for $n\alpha > -1$. For $-1 < n\alpha < 1$, an analytic continuation into the complex is implicitly understood, leading to a replacement of the term $\operatorname{arcosh}(n\alpha)((n\alpha)^2 - 1)^{-3/2}$ by $[-\arccos(n\alpha)](1 - (n\alpha)^2)^{-3/2}$ here and in the following. This leads to the convergent series

$$\mathfrak{I}(\alpha) = \frac{\alpha}{\pi} + \frac{2}{\pi} \sum_{n=1}^{\infty} \left[\frac{-\alpha}{(n\alpha)^2 - 1} + \frac{n\alpha^2 \operatorname{arcosh}(n\alpha)}{((n\alpha)^2 - 1)^{\frac{3}{2}}} \right] \quad (\text{C6})$$

for any $\alpha \geq 0$. Neglecting orders higher than $\frac{1}{\alpha}$ and using $\operatorname{arcosh}(n\alpha) \rightarrow \ln(2n\alpha)$ for $n\alpha \rightarrow \infty$, we arrive at

$$\mathfrak{I}(\alpha) \simeq \frac{\alpha}{\pi} + \frac{\pi \ln \alpha}{3 \alpha} + \frac{\pi}{3} \left(1 + \gamma - \ln \frac{A^{12}}{\pi} \right) \frac{1}{\alpha}, \quad (\text{C7})$$

where $\gamma \approx 0.577$ is the Euler-Mascheroni constant and $A \approx 1.282$ is the Glaisher-Kinkelin constant. The accuracy of this result is above 99% for $\alpha > 5$.

With the series (C6) it is possible to find a series representation for the required integral (43)

$$\mathfrak{F}(\alpha) = \frac{\ln \alpha}{\pi} + \frac{2}{\pi} \sum_{n=1}^{\infty} \left[\ln(2n\alpha) - \frac{n\alpha \operatorname{arcosh}(n\alpha)}{\sqrt{(n\alpha)^2 - 1}} \right]. \quad (\text{C8})$$

This series is convergent for any $\alpha > 0$. The expansions for small and large α are

$$\alpha \rightarrow 0 : \quad \mathfrak{F}(\alpha) \simeq -\frac{1}{\alpha} + c + \frac{\alpha}{12} - \frac{\alpha^3}{240}, \quad (\text{C9})$$

$$\alpha \rightarrow \infty : \quad \mathfrak{F}(\alpha) \simeq \frac{\ln \alpha}{\pi} - \frac{\pi \ln \alpha}{6 \alpha^2}, \quad (\text{C10})$$

where c is defined as the limit

$$c = \lim_{\alpha \rightarrow 0} \left(\mathfrak{F}(\alpha) + \frac{1}{\alpha} \right) \approx 0.364. \quad (\text{C11})$$

[1] V. P. Gusynin, V. A. Miransky and I. A. Shovkovy, Phys. Rev. D **52**, 4718 (1995) [hep-th/9407168].

[2] V. P. Gusynin, V. A. Miransky and I. A. Shovkovy, Phys.

- Lett. B **349**, 477 (1995) [hep-ph/9412257].
- [3] V. P. Gusynin, V. A. Miransky and I. A. Shovkovy, Nucl. Phys. B **462**, 249 (1996) [hep-ph/9509320].
- [4] I. A. Shovkovy, arXiv:1207.5081 [hep-ph].
- [5] I. A. Shushpanov and A. V. Smilga, Phys. Lett. B **402**, 351 (1997) [hep-ph/9703201].
- [6] T. D. Cohen, D. A. McGady and E. S. Werbos, Phys. Rev. C **76**, 055201 (2007) [arXiv:0706.3208 [hep-ph]].
- [7] A. V. Zayakin, JHEP **0807**, 116 (2008) [arXiv:0807.2917 [hep-th]].
- [8] A. J. Mizher, M. N. Chernodub and E. S. Fraga, Phys. Rev. D **82**, 105016 (2010) [arXiv:1004.2712 [hep-ph]].
- [9] R. Gatto and M. Ruggieri, Phys. Rev. D **82**, 054027 (2010) [arXiv:1007.0790 [hep-ph]].
- [10] J. K. Boomsma and D. Boer, Phys. Rev. D **81**, 074005 (2010) [arXiv:0911.2164 [hep-ph]].
- [11] G. S. Bali, F. Bruckmann, G. Endrodi, Z. Fodor, S. D. Katz and A. Schafer, Phys. Rev. D **86**, 071502 (2012) [arXiv:1206.4205 [hep-lat]].
- [12] G. W. Semenoff, I. A. Shovkovy and L. C. R. Wijewardhana, Mod. Phys. Lett. A **13**, 1143 (1998) [hep-ph/9803371].
- [13] K. Krishana, N. P. Ong, Y. Zhang, *et al.*, Phys. Rev. Lett. **82**, 5108 (1999) [cond-mat/9904138].
- [14] D. V. Khveshchenko and W. F. Shively, Phys. Rev. B **73**, 115104 (2006) [cond-mat/0510519].
- [15] D. V. Khveshchenko, Phys. Rev. Lett. **87**, 206401 (2001) [cond-mat/0106261].
- [16] H. Leal and D. V. Khveshchenko, Nucl. Phys. B **687**, 323 (2004) [cond-mat/0302164].
- [17] I. F. Herbut and B. Roy, Phys. Rev. B **77**, 245438 (2008) [arXiv:0802.2546 [cond-mat.mes-hall]]; B. Roy and I. F. Herbut, Phys. Rev. B **83**, 195422 (2011) [arXiv:1102.3481 [cond-mat.mes-hall]].
- [18] E. J. Ferrer and V. de la Incera, Phys. Rev. Lett. **102**, 050402 (2009) [arXiv:0807.4744 [hep-ph]]; Nucl. Phys. B **824**, 217 (2010) [arXiv:0905.1733 [hep-ph]]; E. J. Ferrer, V. de la Incera and A. Sanchez, Phys. Rev. Lett. **107**, 041602 (2011) [arXiv:1103.5152 [hep-ph]].
- [19] D. D. Scherer and H. Gies, Phys. Rev. B **85**, 195417 (2012) [arXiv:1201.3746 [cond-mat.str-el]].
- [20] K. Fukushima and J. M. Pawłowski, Phys. Rev. D **86**, 076013 (2012) [arXiv:1203.4330 [hep-ph]].
- [21] I. L. Buchbinder and E. N. Kirillova, Sov. Phys. J. **32**, 446 (1989); Int. J. Mod. Phys. A **4**, 143 (1989).
- [22] I. L. Buchbinder, S. D. Odintsov and I. L. Shapiro, “Effective action in quantum gravity,” Bristol, UK: IOP (1992).
- [23] T. Inagaki, T. Muta and S. D. Odintsov, Mod. Phys. Lett. A **8**, 2117 (1993) [hep-th/9306023].
- [24] I. Sachs and A. Wipf, Phys. Lett. B **326**, 105 (1994) [hep-th/9310085].
- [25] E. Elizalde, S. Leseduarte, S. D. Odintsov and Y. I. Shil’nov, Phys. Rev. D **53**, 1917 (1996) [hep-th/9505065].
- [26] S. Kanemura and H. -T. Sato, Mod. Phys. Lett. A **11**, 785 (1996) [hep-th/9511059].
- [27] T. Inagaki, Int. J. Mod. Phys. A **11**, 4561 (1996) [hep-th/9512200].
- [28] T. Inagaki and K. -i. Ishikawa, Phys. Rev. D **56**, 5097 (1997).
- [29] B. Geyer and S. D. Odintsov, Phys. Lett. B **376**, 260 (1996) [hep-th/9603172]; Phys. Rev. D **53**, 7321 (1996) [hep-th/9602110].
- [30] G. Miele and P. Vitale, Nucl. Phys. B **494**, 365 (1997) [hep-th/9612168]; P. Vitale, Nucl. Phys. B **551**, 490 (1999) [hep-th/9812076].
- [31] T. Inagaki, T. Muta and S. D. Odintsov, Prog. Theor. Phys. Suppl. **127**, 93 (1997) [hep-th/9711084].
- [32] J. Hashida, S. Mukaigawa, T. Muta, K. Ohkura and K. Yamamoto, Phys. Rev. D **61**, 044015 (2000) [gr-qc/9907014].
- [33] E. V. Gorbar and V. P. Gusynin, Annals Phys. **323**, 2132 (2008) [arXiv:0710.2292 [hep-ph]].
- [34] M. Hayashi, T. Inagaki and H. Takata, arXiv:0812.0900 [hep-ph]; T. Inagaki and M. Hayashi, arXiv:1003.1173 [hep-ph].
- [35] S. Sasagawa and H. Tanaka, Prog. Theor. Phys. **128**, 925 (2012) [arXiv:1209.2782 [hep-ph]].
- [36] E. V. Gorbar, Phys. Rev. D **61**, 024013 (2000) [hep-th/9904180]; Ukr. J. Phys. **54**, 541 (2009) [arXiv:0809.2558 [hep-th]].
- [37] D. Ebert, A. V. Tyukov and V. C. Zhukovsky, Phys. Rev. D **80**, 085019 (2009) [arXiv:0808.2961 [hep-th]].
- [38] D. V. Khveshchenko, Phys. Rev. Lett. **87**, 246802 (2001) [cond-mat/0101306].
- [39] I. F. Herbut, Phys. Rev. Lett. **97**, 146401 (2006) [cond-mat/0606195].
- [40] D. J. Gross and A. Neveu, Phys. Rev. D **10**, 3235 (1974).
- [41] H. A. Weldon, Phys. Rev. D **63**, 104010 (2001) [gr-qc/0009086].
- [42] F. Hofling, C. Nowak and C. Wetterich, Phys. Rev. B **66**, 205111 (2002) [cond-mat/0203588].
- [43] L. Janssen and H. Gies, Phys. Rev. D **86**, 105007 (2012) [arXiv:1208.3327 [hep-th]]; H. Gies and L. Janssen, Phys. Rev. D **82**, 085018 (2010) [arXiv:1006.3747 [hep-th]].
- [44] L. Janssen, “Critical phenomena in (2+1)-dimensional relativistic fermion systems,” PhD Thesis, FSU Jena, <http://www.db-thueringen.de/servlets/DocumentServlet?id=20856> (2012).
- [45] J. Braun, H. Gies and D. D. Scherer, Phys. Rev. D **83**, 085012 (2011) [arXiv:1011.1456 [hep-th]].
- [46] C. Wetterich, Phys. Lett. B **301**, 90 (1993).
- [47] J. Berges, N. Tetradis and C. Wetterich, Phys. Rept. **363**, 223 (2002) [hep-ph/0005122].
- [48] K. Aoki, Int. J. Mod. Phys. B **14**, 1249 (2000).
- [49] J. M. Pawłowski, Ann. Phys. **322**, 2831 (2007) [hep-th/0512261].
- [50] H. Gies, Lect. Notes Phys. **852**, 287 (2012) [hep-ph/0611146].
- [51] B. Delamotte, Lect. Notes Phys. **852**, 49 (2012) [cond-mat/0702365 [COND-MAT]].
- [52] P. Kopietz, L. Bartosch and F. Schutz, Lect. Notes Phys. **798**, 1 (2010).
- [53] W. Metzner, M. Salmhofer, C. Honerkamp, V. Meden and K. Schonhammer, Rev. Mod. Phys. **84**, 299 (2012) [arXiv:1105.5289 [cond-mat.str-el]].
- [54] J. Braun, J. Phys. G **39**, 033001 (2012) [arXiv:1108.4449].
- [55] R. Camporesi, Commun. Math. Phys. **148**, 283 (1992).
- [56] I. S. Gradshteyn and I. M. Ryzhik, “Table of Integrals, Series, and Products,” New York, US: Academic Press (2000).
- [57] J. Jaeckel and C. Wetterich, Phys. Rev. D **68**, 025020 (2003) [hep-ph/0207094].
- [58] U. Ellwanger and C. Wetterich, Nucl. Phys. B **423**, 137 (1994) [hep-ph/9402221].
- [59] H. Gies and C. Wetterich, Phys. Rev. D **65**, 065001

- (2002) [hep-th/0107221].
- [60] V. Skokov, Phys. Rev. D **85**, 034026 (2012) [arXiv:1112.5137 [hep-ph]].
 - [61] J. Braun, C. S. Fischer and H. Gies, Phys. Rev. D **84**, 034045 (2011) [arXiv:1012.4279 [hep-ph]].
 - [62] V. P. Gusynin and S. G. Sharapov, Phys. Rev. Lett. **95**, 146801 (2005) [cond-mat/0506575].
 - [63] D. Nelson, T. Piran and S. Weinberg, “Statistical Mechanics Of Membranes And Surfaces,” Singapore, SG: World Scientific (1989).
 - [64] F. Guinea, M. I. Katsnelson and A. K. Geim, Nature Phys. **6**, 30 (2010) [arXiv:0909.1787 [cond-mat.mes-hall]]; F. Guinea, A. K. Geim, M. I. Katsnelson, K. S. Novoselov, Phys. Rev. B **81**, 035408 (2010); N. Levy *et al.*, Science **329**, 544 (2010).
 - [65] S. Weinberg, In *Hawking, S.W., Israel, W.: General Relativity**, 790-831; M. Reuter, Phys. Rev. D **57**, 971 (1998) [arXiv:hep-th/9605030]; M. Niedermaier and M. Reuter, Living Rev. Rel. **9**, 5 (2006); R. Percacci, In **Orti, D. (ed.): Approaches to quantum gravity** 111-128 [arXiv:0709.3851 [hep-th]]; M. Reuter and F. Saueressig, New J. Phys. **14**, 055022 (2012) [arXiv:1202.2274 [hep-th]].
 - [66] P. Dona and R. Percacci, arXiv:1209.3649 [hep-th]; U. Harst and M. Reuter, JHEP **1205**, 005 (2012) [arXiv:1203.2158 [hep-th]]; R. Percacci and D. Perini, Phys. Rev. D **67**, 081503 (2003) [hep-th/0207033].
 - [67] O. Lauscher and M. Reuter, JHEP **0510**, 050 (2005) [hep-th/0508202].
 - [68] A. Eichhorn and H. Gies, New J. Phys. **13**, 125012 (2011) [arXiv:1104.5366 [hep-th]].